UNSTEADY-STATE FLOW

IN NON-UNIFORM PETROLEUM RESERVOIRS

By

Roy L. Woods

Bachelor of Science

Oklahoma State University of Agriculture and Applied Science

Stillwater, Oklahoma

1960

Submitted to the Faculty of the Graduate School of
the Oklahoma State University of Agriculture and
Applied Science in partial fulfillment of the
requirements for the degree of
MASTER OF SCIENCE
August, 1961

UNSTEADY-STATE FLOW

IN NON-UNIFORM PETROLEUM RESERVOIRS

Thesis Approved:

David Cornell

Thesis Adviser

J. H. Boggs

Robert MacVicar

Dean of the Graduate School

ACKNOWLEDGEMENT

I am grateful to the Pan American Foundation, Inc. for providing the graduate fellowship which made this study possible. I wish to express my appreciation to my adviser, Dr. David Cornell, for the help and guidance he gave me, to Professor William Granet for his helpful suggestions on programing methods and to the Computing Center for permitting me to use their computing machines.

The assistance Mrs. Mildred Avery gave in the typing of the manuscript and the help Mr. John Rogers rendered in preparing the figures is also greatly appreciated.

TABLE OF CONTENTS

LIST OF FIGURES

LIST OF TABLES

NOMENCLATURE

P	dimensionless pressure ratio
P_t	dimensionless pressure change function
p	pressure, psia.
$\bar{p}$	average pressure, psia.
p_f	shut-in reservoir pressure, psia.
R	dimensionless radius
R_1	radius of inner zone, dimensionless
r_w	radius of well bore, feet
r	radial distance, feet
ΔR_1	pivotal-point spacing of inner zone, dimensionless
ΔR_2	pivotal-point spacing of outer zone, dimensionless
t_D	dimensionless time
t	time, hours
Δt_D	dimensionless time increment
Δt	time increment, hours
T	temperature of reservoir, degrees Rankine
q_D	dimensionless flow rate
Q	flow rate, Mcf/day
K	permeability, millidarcys
K_1	permeability of inner zone, millidarcys
K_2	permeability of outer zone, millidarcys

μ	viscosity, centipoises
$\overline{\mu}$	average viscosity, centipoises
$\overline{Z}$	average compressibility factor
S	slope of draw-down curve, psia./cycle
h	reservoir thickness, feet
N	number of incremental time steps
D	percent deviation between calculated values and accepted values
ϕ	porosity, fractional

FORTRAN PROGRAM SYMBOLS

P	dimensionless pressure ratio, floating-point number
KQD	dimensionless flow rate
KDRK1	pivotal-point spacing of inner zone
KDRK2	pivotal-point spacing of outer zone
KRK1Z	radius of inner zone
N	number of incremental time steps
KDRI	incrementing factor
IKR	number of the pivotal point at the boundary between the two zones
NPC	number of calculations
L	control parameter
IOB	number of the pivotal point at the outer boundary
M	incrementing factor
A	floating-point constant

QD	dimensionless flow rate, floating-point number
DRK1	pivotal-point spacing of inner zone, floating-point number
DRK2	pivotal-point spacing of outer zone, floating-point number
RK1Z	radius of inner zone, floating-point number
DRI	incrementing factor, floating-point number
AIKR	number of the pivotal point at boundary between the two zones, floating-point number
AN	number of incremental time steps, floating-point number
K	calculation number
J	control parameter
T	constant
W	constant
X	constant
Y	constant
S	constant
IMAX	number of the outermost pivotal point which the pressure transient has reached
AI	number of pivotal point
RO	distance to outer pivotal point
RI	distance to pivotal point of calculation
RN	distance to inner pivotal point
B	constant
C	constant
TD	dimensionless time, floating point number
PT	dimensionless pressure change function, floating point number

APR	constant
CPR	constant
DEV	deviation between calculated pressure and accepted value, floating-point number
KTD	dimensionless time
DP	dimensionless pressure ratio
KPT	dimensionless pressure change function
KDE	deviation
BIKR	constant
BDRK1	constant

CHAPTER I

INTRODUCTION

The hydraulic fracturing of a petroleum reservoir alters the physical properties of the reservoir by creating flow channels of increased permeability in the area adjacent to the well bore. The petroleum industry is interested in determining the effective fracture radius and the increase in effective permeability created by different hydraulic fracturing procedures. Bottom-hole pressure tests have been used to determine the effective permeability of reservoirs; but, the theory which has been developed assumes the reservoir to be of uniform permeability. In the fractured reservoir, this condition does not exist.

The effect of hydraulic fracturing on a petroleum reservoir has been approximated mathematically by assuming the reservoir is composed of two, radial, concentric zones of different permeabilities. (6). This theoretical representation of a fractured reservoir is schematically depicted by Figure 1.

In this study a mathematical reservoir model composed of two concentric zones of different permeability was used to approximate a fractured reservoir. The inner and outer zones of the reservoir have uniform permeabilities of K_1 and K_2 respectively. The radial

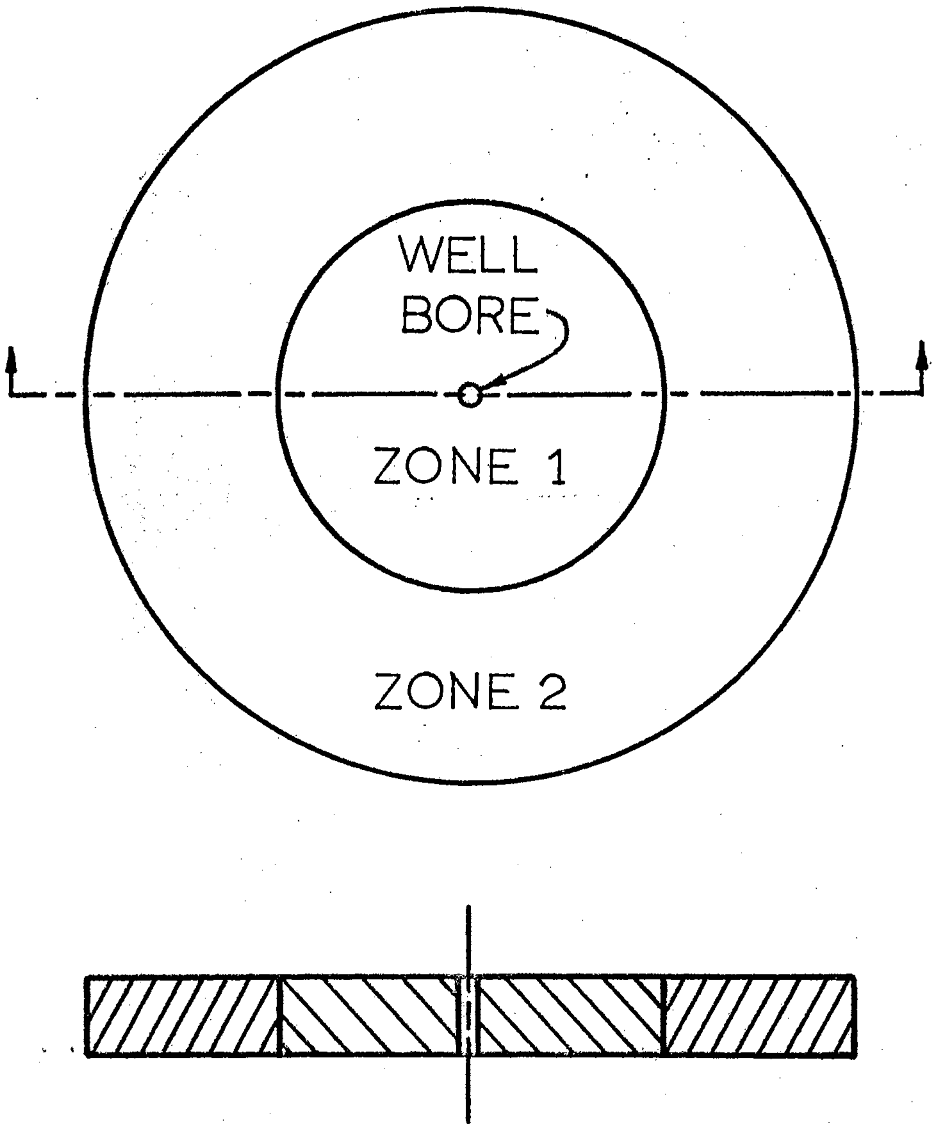

FIGURE 1 RESERVOIR MODEL

extent of the reservoir was assumed to be infinite. The reservoir was initially assumed to be at a uniform pressure; then a constant flow rate was produced across the inner boundary.

The imposed flow rate created two pressure transients in the reservoir. The pressure transients were determined by using a digital computer to solve difference equations developed for fluid flow in the system. By calculating the pressure at the inner boundary, pressure draw-down curves were obtained.

The draw-down curves were analyzed to determine the effect of the two transients on the pressure at the inner boundary of the reservoir. From the analysis a procedure was developed for calculating the radius and permeability of the inner zone from a draw-down curve. A set of curves was prepared for estimating the permeability of the outer zone.

CHAPTER II

PREVIOUS INVESTIGATIONS

Many single phase unsteady-state flow problems have been studied. Most of the investigations are for finite and infinite reservoirs with uniform permeability. Very little literature has been published for unsteady-state flow in petroleum reservoirs with non-uniform properties. Only a few of the more significant contributions and those articles which directly pertain to this study will be discussed.

Muskat (12) derived a point source solution in terms of an exponential integral for determining the unsteady-state pressure distribution in a petroleum reservoir. Horner (7) later used the point source solution to calculate pressure build-up curves. A procedure was presented for determining the permeability of the reservoir from the slope of the build-up curve. A method was also given for extrapolating build-up curves to obtain the shut-in reservoir pressure. The cases of finite and infinite reservoirs were studied.

Just previous to Horner's work, Miller, Dyes and Hutchinson (10) presented a similar procedure for calculating the effective permeability of a reservoir from the slope of the pressure build-up curve. Their theory was developed from a Fourier-Bessel solution of the radial flow equation. The effect of after flow and of improved and decreased permeability in area around the well bore was studied.

Van Everdingen and Hurst (15) presented a procedure for solving the radial unsteady-state flow equation by using Laplace transformations. By introducing dimensionless groups, curves and tables were compiled from which the bottom-hole pressure after any flow period could be determined in a uniform reservoir. For dimensionless time values greater than 100, equation (2-1) which was derived from the point source solution was found to give accurate results.

$$P_t = \tfrac{1}{2}[\ln(t_D) + 0.80907] \qquad (2\text{-}1)$$

where

P_t = Dimensionless pressure change function

t_D = Dimensionless time

Chatas (1) later expanded upon the work of Van Everdingen and Hurst. Graphs and tables for calculating well bore pressures in a variety of finite reservoir cases were developed.

Cornell and Katz (3) applied the Schmidt method for graphical solution of heat flow problems to fluid flow in natural gas reservoirs. The radial unsteady-state flow equation was converted into finite difference form and integrated graphically to obtain the well bore pressure. The effect of turbulence at the well bore was also included.

Cornell (2) presented a procedure for determining the effective permeability of a reservoir from the draw-down curve for the constant production rate case. A plot of p^2 versus the logarithm of t was made. The slope of the curve was used to evaluate the permeability by using equation (2-2).

$$K = \frac{1,424\ \bar{\mu}\ \bar{Z}\ T\ Q}{2\ h\ S} \tag{2-2}$$

where

K = Permeability, millidarcys

$\bar{\mu}$ = Average viscosity, centipoises

$\bar{Z}$ = Average compressibility factor

T = Temperature of reservoir, degrees Rankine

Q = Flow rate, Mcf/day

h = Reservoir thickness, feet

S = Slope of curve divided by 2.303, psia^2/cycle

Mortada (11) recently published an analysis of the interference pressure drop for oil fields located in a non-uniform aquifer. Loucks (9) has derived an equation in terms of Bessel functions for calculating build-up pressures in composite reservoirs. Because of the lack of computing facilities, the equation was not evaluated. No literature has yet been published on pressure draw-down curves for unsteady-state fluid flow in composite reservoirs.

CHAPTER III

DIMENSIONLESS GROUPS

Dimensionless groups are used in petroleum reservoir analysis to take advantage of the principle of similitude; two different physical systems described by equivalent dimensionless groups will perform in a similar manner. The dimensionless groups which have been presented (8) for describing the properties and producing characteristics of natural gas reservoirs were employed in this study. Equivalent dimensionless groups for single phase flow in oil reservoirs may also be used.

Five dimensionless groups were used in this study. They are dimensionless time, dimensionless radial distance, dimensionless flow rate, dimensionless pressure ratio and dimensionless pressure change function.

Dimensionless time expresses the relationship between time, permeability, average pressure, viscosity, porosity and well bore radius. In field units the dimensionless time is written as follows:

$$t_D = \frac{2.634 \times 10^{-4}\ t\ K\ \bar{p}}{\mu\ \phi\ r_w^{\,2}} \tag{3-1}$$

where

t_D = Dimensionless time

t = Time, hours

K = Permeability, millidarcys

$\overline{p}$ = Average pressure, psia

μ = Viscosity, centipoises

ϕ = Porosity, fractional

r_w = Radius of well bore, feet

The dimensionless radius is the radial distance from the center of the well bore to a point in the reservoir divided by the well bore radius. The dimensionless radius in equation form is as follows:

$$R = \frac{r}{r_w} \tag{3-2}$$

where

R = Dimensionless radius

r = Radial distance, feet

r_w = Radius of well bore, feet

Dimensionless flow rate expresses the relationship between the flow rate, average viscosity, average compressibility factor, temperature of the reservoir, formation thickness, permeability and shut-in formation pressure. This group is related to the slope of the steady state pressure gradient. In field units the dimensionless flow rate is expressed as follows:

$$q_D = \frac{1,424 \, Q \, \overline{\mu} \, \overline{Z} \, T}{h \, K \, p_f^2} \tag{3-3}$$

where

q_D = Dimensionless flow rate

Q = Flow rate, Mcf/day

$\overline{\mu}$ = Average viscosity, centipoises

$\bar{Z}$ = Average compressibility factor

T = Temperature of reservoir, degrees Rankine

K = Permeability, millidarcys

h = Reservoir thickness, feet

p_f = Shut-in reservoir pressure, psia.

The dimensionless pressure ratio represents the fractional decrease in pressure at a given position and time in the reservoir. In equation form the dimensionless pressure ratio is written as follows:

$$P = \frac{p^2}{{p_f}^2} \qquad (3\text{-}4)$$

where

P = Dimensionless pressure ratio

p = Pressure in reservoir, psia.

p_f = Shut-in reservoir pressure, psia.

The dimensionless pressure change function is a dimensionless value which relates the dimensionless pressure ratio to the dimensionless flow rate. The relationship is expressed as follows:

$$P_t = \frac{P-1}{q_D} \qquad (3\text{-}5)$$

where

P_t = Dimensionless pressure change function

P = Dimensionless pressure ratio

q_D = Dimensionless flow rate

The equations developed in Chapter V and all numerical calculations were made in terms of these dimensionless groups.

CHAPTER IV

MATHEMATICAL ANALYSIS

Unsteady-state radial flow in a porous media is defined mathematically by an equation which will relate pressure with position and time. An equation of this type can be derived by using Darcy's Law (5) and the principle of conservation of mass.

The pressure distribution for radial flow has been derived by many authors. For natural gas reservoirs, the equation for radial flow in dimensionless form is given by equation (4-1). (8).

$$\frac{\partial^2 P}{\partial R^2} + \frac{1}{R}\frac{\partial P}{\partial R} = \frac{\partial P}{\partial t_D} \tag{4-1}$$

where

P = Dimensionless pressure

R = Dimensionless radius

t_D = Dimensionless time

Equation (4-1) has been solved by finite differences. (3). The finite difference scheme is illustrated in Figure 2.

The second partial of P with respect to R is replaced by central differences. (13).

$$\frac{\partial^2 P}{\partial R^2} = \frac{P(i+1,t_D) - 2P(i,t_D) + P(i-1,t_D)}{(\Delta R)^2} \tag{4-2}$$

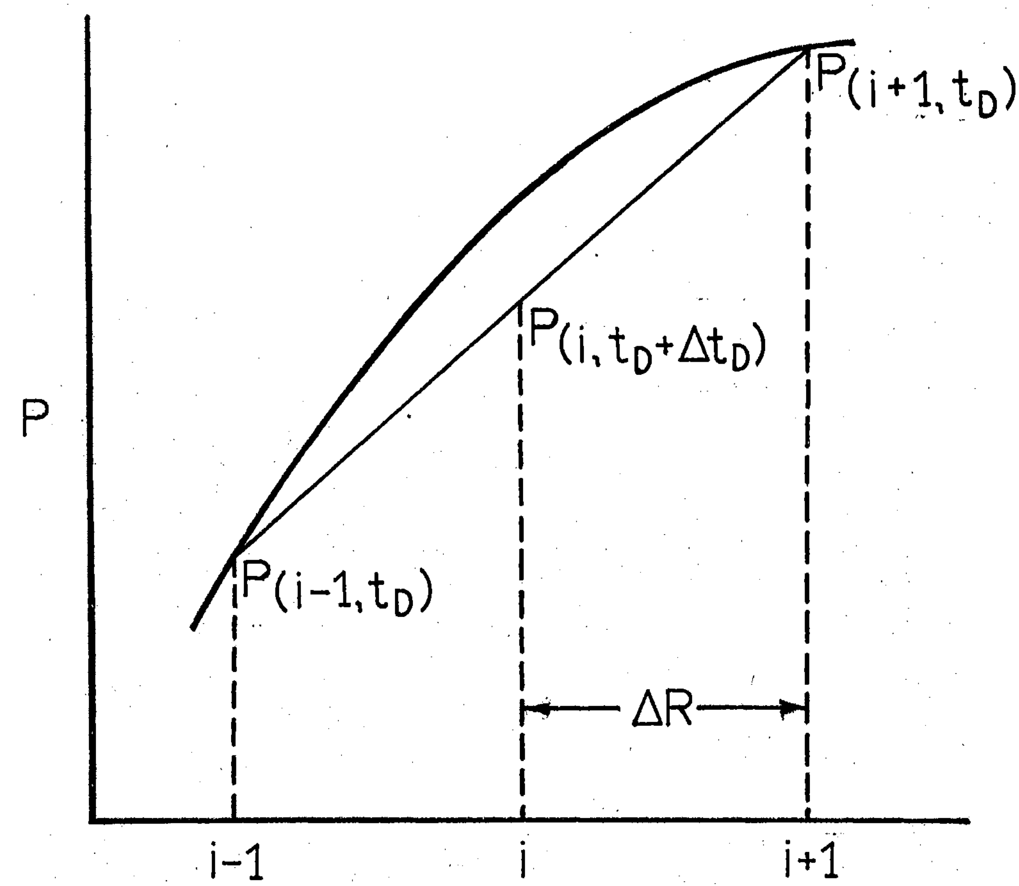

FIGURE 2 DIFFERENCE SCHEME

The subscripts "i" and "t_D" on P, as indicated by parentheses, denote the dimensionless pressure at the "ith" pivotal point at a dimensionless time of t_D. The term ΔR is the dimensionless distance between pivotal points.

The first partial of P with respect to R is also replaced by central differences.

$$\frac{\partial P}{\partial R} = \frac{P(i+1,t_D) - P(i-1,t_D)}{2(\Delta R)} \tag{4-3}$$

The partial of P with respect to t_D is replaced by a forward difference. (13).

$$\frac{\partial P}{\partial t_D} = \frac{P(i,t_D+\Delta t_D) - P(i,t_D)}{\Delta t_D} \tag{4-4}$$

The term Δt_D denotes the incremental change in dimensionless time.

When the differences are substituted for the partial differentials, equation (4-1) takes the form given by equation (4-5).

$$\frac{P(i+1,t_D)-2P(i,t_D)+P(i-1,t_D)}{(\Delta R)^2}+\frac{1}{R}\,\frac{P(i+1,t_D)-P(i-1,t_D)}{2(\Delta R)} = \frac{P(i,t_D+\Delta t_D)-P(i,t_D)}{\Delta t_D} \tag{4-5}$$

To insure convergence, the ratio of $(\Delta R)^2/\Delta t_D$ must be equal to or greater than two. (14). The ratio $(\Delta R)^2/\Delta t_D$ is set equal to two in order to facilitate the cancellation of the $P(i,t_D)$ term. With this substitution, equation (4-5) takes the form given by equation (4-6). (3).

$$P(i, t_D + \Delta t_D) = [(1 - \Delta R/2R)\ P(i-1, t_D) + \qquad (4\text{-}6)$$

$$(1 + \Delta R/2R)\ P(i+1, t_D)]/2$$

The finite difference method assumes a succession of incremental steady-state flows to approximate unsteady-state flow. By directly integrating the steady-state flow equation and substituting the result into the finite difference scheme, a closer approximation was obtained.

The steady-state flow equation or Darcy's Law in dimensionless form is given by equation (4-7). (5).

$$q_D = R \frac{dP}{dR} \qquad (4\text{-}7)$$

Integration of equation (4-7) yields equation (4-8).

$$P_2 - P_1 = q_D \ln \frac{R_2}{R_1} \qquad (4\text{-}8)$$

Equation (4-8) may be written in the form of equations (4-9) and (4-10).

$$P(i-1) + q_D \ln \frac{R(i)}{R(i-1)} = P_{(i)} \qquad (4\text{-}9)$$

$$P(i+1) - q_D \ln \frac{R(i+1)}{R(i)} = P_{(i)} \qquad (4\text{-}10)$$

By subtracting equation (4-9) from equation (4-10) and solving for q_D, equation (4-11) is obtained.

$$q_D = [P(i+1) - P(i-1)] \ / \ \ln \frac{R(i+1)}{R(i-1)} \qquad (4\text{-}11)$$

The substitution of q_D from equation (4-11) into equation (4-9) gives equation (4-12).

$$P(i) = \left[\ln \frac{R(i+1)}{R(i)} P(i-1) + \ln \frac{R(i)}{R(i-1)} P(i+1)\right] \Big/ \ln \frac{R(i+1)}{R(i-1)} \tag{4-12}$$

By using the forward difference scheme to include time, equation (4-12) takes the form given by equation (4-13).

$$P(i,\ t_D+\Delta t_D) = \left[\ln \frac{R(i+1)}{R(i)} P(i-1,t_D) + \ln \frac{R(i)}{R(i-1)} P(i+1,t_D)\right] \Big/ \ln \frac{R(i+1)}{R(i-1)} \tag{4-13}$$

Both equations (4-6) and (4-13) were incorporated into computer programs for calculating well bore pressures. The answers obtained from the computer program incorporating equation (4-13) were in closer agreement with the Van Everdingen and Hurst solutions than the answers from the computer program incorporating equation (4-6).

In the derivation of the difference equation, $(\Delta R)^2/\Delta t_D$ was set equal to two. Solving for ΔR gives equation (4-14).

$$\Delta R = \left[\frac{2 \times 2.634 \times 10^{-4}\ K\ \bar{p}\ \Delta t}{\mu\ \phi\ r_w^2}\right]^{\frac{1}{2}} \tag{4-14}$$

where

K = Permeability, millidarcys

$\bar{p}$ = Average pressure, psia.

Δt = Time increment, hours

μ = Viscosity, centipoises

ϕ = Porosity, fractional

r_w = Radius of well bore, feet

By changing K to K_2 and holding Δt constant, a different value of ΔR is obtained. From this relationship the procedure for representing the two zones of different permeabilities was developed. The inner and outer zones were mathematically represented by pivotal point spacing of ΔR_1 and ΔR_2 respectively.

By using the theory which has been presented, a procedure was developed to cross the boundary between the zones of different permeabilities. Figure 3 shows schematically the procedure used. The boundary conditions are a constant flow rate across the zone of contact and a pressure, $P_{(i)}$, common to both zones. Using these boundary conditions, equations (4-9) and (4-10) take the form of equations (4-15) and (4-16).

$$P(i) = P(i+1) + q_{D_1} \ln \frac{R(i)}{R(i-1)} \tag{4-15}$$

$$P(i) = P(i-1) - q_{D_2} \ln \frac{R(i+1)}{R(i)} \tag{4-16}$$

The terms q_{D_1} and q_{D_2} are given by equations (4-17) and (4-18).

$$q_{D_1} = \frac{1,424\, \bar{\mu}\, \bar{Z}\, T\, Q}{h\, K_1\, P_f^2} \tag{4-17}$$

$$q_{D_2} = \frac{1,424\, \bar{\mu}\, \bar{Z}\, T\, Q}{h\, K_2\, P_f^2} \tag{4-18}$$

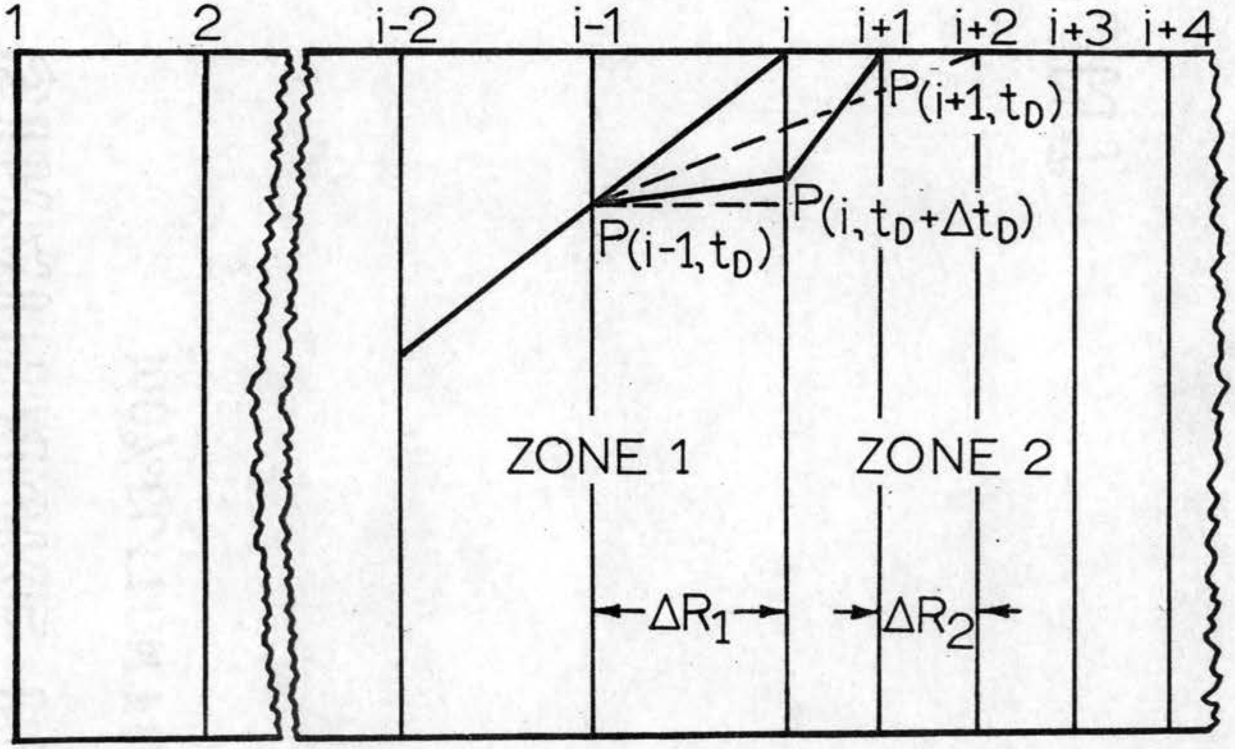

FIGURE 3 MATHEMATICAL MODEL

Where

$\bar{\mu}$ = Average viscosity, centipoises

$\bar{Z}$ = Average compressibility factor

T = Temperature of reservoir, degrees Rankine

Q = Flow rate across boundary, Mcf/day

h = Reservoir thickness, feet

p_f = Shut-in reservoir pressure, psia.

K_1 = Permeability of inner zone, millidarcys

K_2 = Permeability of outer zone, millidarcys

The dimensionless flow rate q_{D_2} is obtained by dividing equation (4-18) by equation (4-17) and rearranging terms. Equation (4-19) gives q_{D_2}.

$$q_{D_2} = \frac{K_1\, q_{D_1}}{K_2} \tag{4-19}$$

By subtracting equation (4-15) from equation (4-16) and substituting equation (4-19) for q_{D_2}, equation (4-20) is obtained.

$$q_{D_1} = [P(i+1)-P(i-1)]/[\ln \frac{R(i)}{R(i-1)} + \frac{K_1}{K_2} \ln \frac{R(i+1)}{R(i)}] \tag{4-20}$$

The substitution of equation (4-20) into equation (4-15) gives equation (4-21).

$$P(i) = [\frac{K_1}{K_2} \quad \frac{R(i+1)}{R(i)} \quad P(i-1) + \ln \frac{R(i)}{R(i-1)} \; P(i+1)] / \tag{4-21}$$
$$[\ln \frac{R(i)}{R(i-1)} + \frac{K_1}{K_2} \ln \frac{R(i+1)}{R(i)}]$$

By using the forward difference scheme to introduce time, equation (4-21) takes the form given by equation (4-22).

$$P(i,\ t_D+\Delta t_D) = \left[\frac{K_1}{K_2} \ln \frac{R(i+1)}{R(i)}\ P(i-1,\ t_D) + \ln \frac{R(i)}{R(i-1)}\ P(i+1,\ t_D)\right] / \left[\ln \frac{R(i)}{R(i-1)} + \frac{K_1}{K_2}\ \ln \frac{R(i+1)}{R(i)}\right] \quad (4\text{-}22)$$

Equation (4-19) reduces to equation (4-13) when K_1 is equal to K_2.

The total elapsed time is equal to the number of incremental time steps taken multiplied by the size of the time increment. This relationship is given by equation (4-23).

$$t = N(\Delta t) \quad (4\text{-}23)$$

where

t = Total time, hours

N = Number of incremental time steps

Δt = Time increment, hours

By using equations (3-1), (4-14) and (4-23), an equation for the total elapsed dimensionless time in terms of the number of incremental time steps taken and the pivotal point spacing is obtained. Equation (4-24) expresses this relationship.

$$t_D = \frac{N}{2}\ (\Delta R)^2 \quad (4\text{-}24)$$

The equations developed in this chapter were used to calculate the pressure draw-down at the inner boundary of the reservoir. Chapter V explains the procedure which was used in making the calculations.

CHAPTER V

CALCULATION PROCEDURE

The equations developed in Chapter IV were incorporated in a 650 Fortran program. All calculations were made on an IBM 650 digital computer. A listing of the program is presented in Table I. A flow chart is presented in Figure 4 to illustrate the basic steps of the program.

First, 300 storage locations were reserved in the memory of the computer. These storage locations represented the pivotal points in the mathematical reservoir model.

The initial data read into the computer were the dimensionless flow rate at the inner boundary of the reservoir, the pivotal point spacing of the inner zone, the pivotal point spacing of the outer zone and the radius of the inner zone. With the initial data, the calculations were made.

The calculation procedure used was similar to the graphical solution method presented by Cornell and Katz (3).

The initial condition of a uniform pressure throughout the reservoir was imposed by setting the pressure ratios at all pivotal points equal to one. A constant flow rate across the inner boundary was then imposed on the reservoir. This condition was imposed by setting the slope of the pressure gradient on the logarithmic distance

TABLE I

THE 650 FORTRAN PROGRAM

```
      DIMENSIONP(300)
  1 0 READ,KQD,KDRK1,KDRK2,KRK1Z,N,K
  1 1 DRI,IKR,NPC,L,IOB,M
  2 0 A=KQD
  3 0 QD=A*0.000001
  4 0 A=KDRK1
  5 0 DRK1=A*0.01
  6 0 A=KDRK2
  7 0 DRK2=A*0.01
  8 0 A=KRK1Z
  9 0 RK1Z=A*0.01+1.0
 10 0 DRI=KDRI
 11 0 AIKR=IKR
 12 0 AN=N
 13 0 K=1
 16 0 CONTINUE
 17 0 J=1
 20 0 DO21I=1,300
 21 0 P(I)=1.0
 25 0 Z=(DRK1/DRK2)**2
 26 0 T=LOGEF((RK1Z+DRK1)/RK1Z)
 27 0 W=Z*T
 28 0 X=LOGEF(RK1Z/(RK1Z-DRK1))
 29 0 Y=W+X
 30 0 S=QD*LOGEF(2.0*DRK1)
 34 0 IMAX=3
 35 0 CONTINUE
 36 0 DO52I=3,IMAX,2
 37 0 IF(I-IMAX)38,52,52
 38 0 AI=I
 39 0 IF(I-IKR)40,44,46
 40 0 RO=AI*DRK1+1.0
 41 0 RI=RO-DRK1
 42 0 RN=RI-DRK1
 43 0 GOTO49
 44 0 P(I)=(W*P(I-1)+X*P(I+1))/Y
 45 0 GOTO52
 46 0 RI=RK1Z+(AI-AIKR)*DRK2
 47 0 RO=RI+DRK2
 48 0 RN=RI-DRK2
 49 0 B=LOGEF(RI/RN)
 50 0 C=LOGEF(RO/RN)
 51 0 P(I)=P(I-1)+(P(I+1)-P(I-1))*B/
 51 1 C
 52 0 CONTUNUE
 53 0 P(1)=P(3)-S
 55 0 IF(IMAX-IOB)56,58,58
 56 0 IMAX=IMAX+1
 57 0 GOTO59
 58 0 P(IOB)=P(IOB-1)
 59 0 CONTINUE
 61 0 DO76I=2,IMAX,2
      IF(I-IMAX)62,76,76
 62 0 AI=I
 63 0 IF(I-IKR)64,68,70
 64 0 RO=AI*DRK1+1.0
 65 0 RI=RO-DRK1
 66 0 RN=RI-DRK1
 67 0 GOTO73
 68 0 P(I)=(W*P(I-1)+X*P(I+1))/Y
 69 0 GOTO76
 70 0 RI=RK1Z+(AI-AIKR)*DRK2
 71 0 RO=RI+DRK2
 72 0 RN=RI-DRK2
 73 0 B=LOGEF(RI/RN)
 74 0 C=LOGEF(RO/RN)
 75 0 P(I)=P(I-1)+(P(I+1)-P(I-1))*B/
 75 1 C
 76 0 CONTUNUE
 78 0 IF(J-N)79,82,82
 79 0 J=J+2
126 0 IF(IMAX-IOB)80,118,118
 80 0 IMAX=IMAX+1
 81 0 GOTO35
118 0 P(IOB)=P(IOB-1)
119 0 GOTO35
 82 0 TD=AN*0.5*DRK1**2
 83 0 PT=0.5*(LOGEF(TD)+0.80907)
 84 0 APR=PT*QD
 85 0 CPR=1.0-P(1)
 86 0 DEV=(APR-CPR)/APR
 87 0 KTD=TD
 88 0 KPT=PT*1000.0
 89 0 KP=P(1)*100000000.0
 90 0 KDE=DEV*10000.0
 91 0 KDRK1=DRK1*100.0
110 0 GOTO(116,111),L
111 0 CONTINUE
121 0 PUNCH,KDRK1,KDRK2,KRK1Z,IKR,IM
121 1 AX,TD,PT
112 0 DO114I=1,300
113 0 PUNCH,I,P(I)
114 0 CONTINUE
115 0 GOTO1
116 0 CONTINUE
 94 0 PUNCH,K,KTD,KP,KPT,KDE,N,KDRK1
 95 0 IF(K-NPC)96,1,1
 96 0 BIKR=(AIKR-1.0)-DRI*1.0
      IKR=BIKR
      IOB=IKR*M+1
 97 0 BDRK1=(RK1Z-1.0)/BIKR
 98 0 DRK2=DRK2*(BDRK1/DRK1)
 99 0 DRK1=BDRK1
100 0 AIKR=BIKR+1.0
101 0 IKR=AIKR
103 0 K=K+1
104 0 GOTO16
105 0 END
```

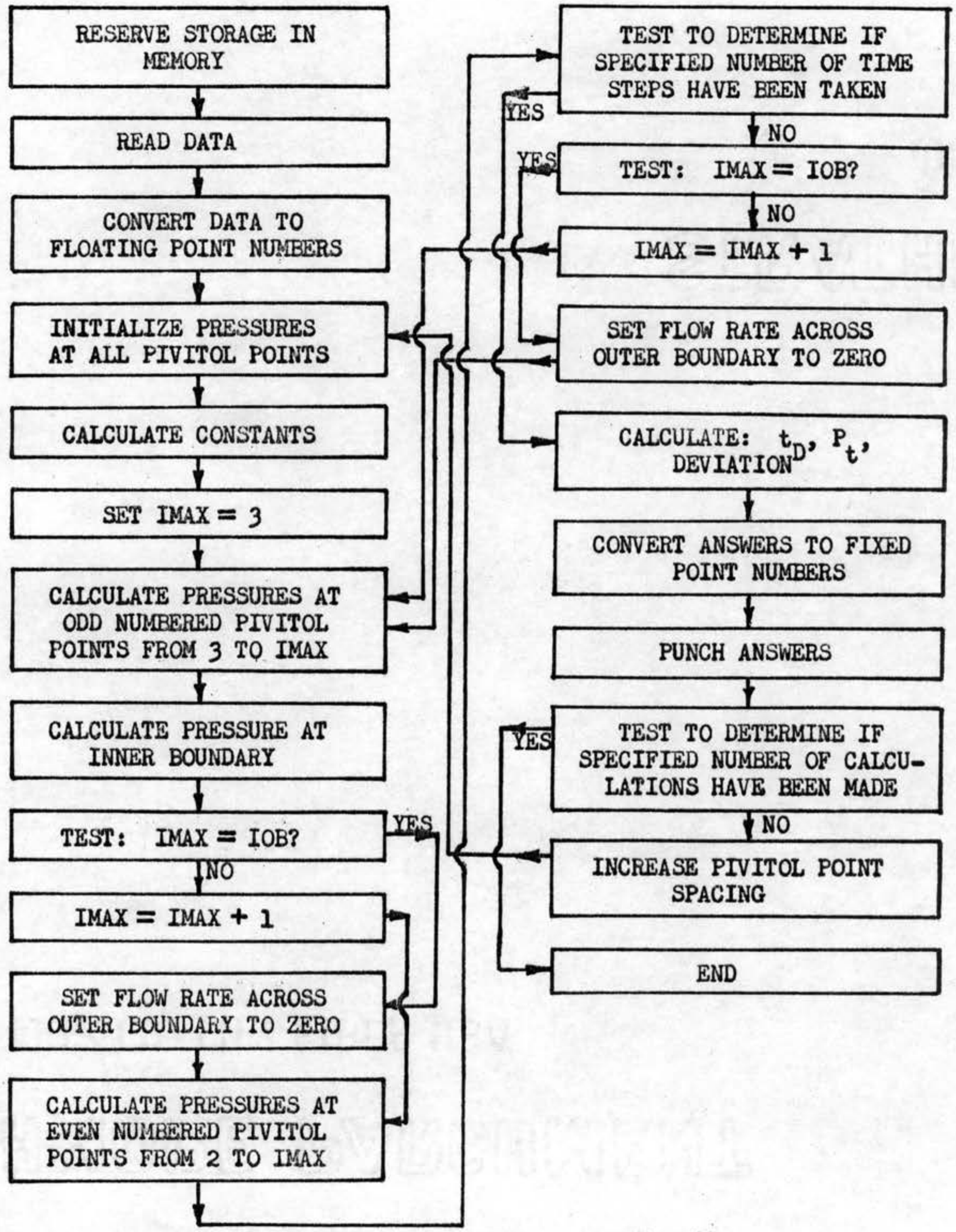

FIGURE 4 FLOW DIAGRAM OF COMPUTER PROGRAM

between pivotal points one and three equal to the dimensionless flow rate across the inner boundary.

Equation (4-13) was used to calculate the pressure transients in the reservoir. The pressure ratios were alternately calculated at successive even and odd numbered pivotal points. The calculations for each set of pivotal points represents an increment in time.

The pressure transient moved outward one pivotal point spacing with each time step. When the pressure transient crossed the boundary between the two zones, equation (4-22) was used to calculate the pressure ratio at the pivotal point on the boundary.

After a specified number of time steps had been taken, the total elapsed dimensionless time, the dimensionless pressure change function and the percent deviation were calculated. The total elapsed dimensionless time was calculated by using equation (4-24). Equation (2-1) was used to calculate the dimensionless pressure change function. The percent deviation between the calculated answers and the Van Everdingen and Hurst solutions was obtained by using equation (5-1).

$$D = \frac{P_t\, q_D - (P-1)}{P_t\, q_D} \times 100 \qquad (5\text{-}1)$$

where

D = Percent deviation

P_t = Dimensionless pressure change function

P = Dimensionless pressure ratio at inner boundary

q_D = Dimensionless flow rate across inner boundary

The pivotal point spacing was increased and the entire calculation procedure was repeated. A new pressure ratio was thus obtained at a larger dimensionless time after the same number of calculations. This resulted in a nearly constant percent deviation between the calculated values and accepted values. The calculation procedure was repeated until a specified number of pressure ratios had been calculated.

For the case of zero permeability in the outer zone, the pressure ratios at the pivotal point on the boundary between the zones and the next inner pivotal point were set equal to each other after every time step. The flow across the boundary was thus set equal to zero.

The calculation procedure requires a vast amount of very accurate calculations; consequently, the only feasible means for making the calculations was on a digital computer.

CHAPTER VI

PRESENTATION OF RESULTS

The answers, obtained for the case of an inner permeability zone with dimensionless radius of 600, are presented in Table II. Similar sets of answers were calculated for reservoirs with inner permeability zones of dimensionless radii equal to 300, 400 and 500.

The values of the pressure ratios calculated at the inner boundary, when the permeability ratio between zones was equal to one, agree very closely with the Van Everdingen and Hurst solutions. The maximum deviation was less than 0.65 percent. For the case of an infinite permeability ratio, the dimensionless pressure ratios calculated agreed within 0.50 percent of answers obtained from an equation developed by Chatas (1).

The results of all cases were made to coincide with one set of curves by properly selecting the dimensionless parameters for the coordinates of the plot. Figure 5 shows a plot of the results. The curves all deviated from a straight line at the same dimensionless value of t_D/R_1^2. The symbol R_1 is used to denote the radius of the inner zone. The plot is for dimensionless times greater than 100 and dimensionless radii of the inner zone greater than 150.

The dimensionless pressure change function was used on one coordinate so the curves could be used for any flow rate. The

TABLE II

COMPUTER PROGRAM ANSWERS

	CAL. NO.	t_D	P	P_t	% DEV.	N	ΔR_1
$\frac{K_1}{K_2}=1.0$	1+	10200+	94963+	5019+	33-	51+	2000+
	2+	10915+	94928+	5053+	35-	51+	2068+
	3+	11709+	94892+	5088+	37-	51+	2142+
	4+	12592+	94854+	5124+	39-	51+	2222+
	5+	13579+	94816+	5162+	40-	51+	2307+
	6+	14688+	94775+	5201+	42-	51+	2400+
	7+	15937+	94734+	5242+	44-	51+	2500+
	8+	17353+	94690+	5285+	45-	51+	2608+
	9+	18966+	94644+	5329+	47-	51+	2727+
	10+	20816+	94597+	5376+	49-	51+	2857+
	11+	22950+	94547+	5425+	50-	51+	3000+
	12+	25429+	94495+	5476+	51-	51+	3157+
	13+	28333+	94440+	5530+	53-	51+	3333+
	14+	31764+	94381+	5587+	54-	51+	3529+
	15+	35859+	94320+	5648+	55-	51+	3750+
	16+	40800+	94254+	5712+	57-	51+	4000+
	17+	46836+	94184+	5781+	58-	51+	4285+
	18+	63750+	94028+	5935+	59-	51+	5000+
	19+	75867+	93940+	6022+	60-	51+	5454+
	20+	91800+	93844+	6118+	61-	51+	6000+
	21+	113333+	93737+	6223+	61-	51+	6666+
	22+	143437+	93619+	6341+	62-	51+	7500+
	23+	187346+	93484+	6474+	62-	51+	8571+
	24+	255000+	93329+	6629+	62-	51+	10000+
	25+	573750+	92922+	7034+	61-	51+	15000+
$\frac{K_1}{K_2}=1.57$	1+	63750+	94027874+	5935+	61-	51+	5000+
	2+	75867+	93938671+	6022+	63-	51+	5454+
	3+	91800+	93839475+	6118+	69-	51+	6000+
	4+	113333+	93726781+	6223+	79-	51+	6666+
	5+	143437+	93595130+	6341+	100-	51+	7500+
	6+	187346+	93436220+	6474+	137-	51+	8571+
	7+	255000+	93237428+	6629+	201-	51+	10000+
	8+	367200+	92979595+	6811+	306-	51+	12000+
	9+	573750+	92632114+	7034+	473-	51+	15000+
$\frac{K_1}{K_2}=16.0$	1+	91800+	93823691+	6118+	94-	51+	6000+
	2+	113333+	93689501+	6223+	139-	51+	6666+
	3+	143437+	93512618+	6341+	230-	51+	7500+
	4+	187346+	93263013+	6474+	404-	51+	8571+
	5+	255000+	92886023+	6629+	731-	51+	10000+
	6+	367200+	92270975+	6811+	1347-	51+	12000+
	7+	573750+	91155898+	7034+	2572-	51+	15000+
$\frac{K_1}{K_2}=\infty$	1+	63750+	94025197+	5935+	65-	51+	5000+
	2+	75867+	93931298+	6022+	76-	51+	5454+
	3+	91800+	93820722+	6118+	99-	51+	6000+
	4+	113333+	93682402+	6223+	151-	51+	6666+
	5+	143437+	93496633+	6341+	255-	51+	7500+
	6+	187346+	93228496+	6474+	458-	51+	8571+
	7+	255000+	92812543+	6629+	842-	51+	10000+
	8+	367200+	92110119+	6811+	1583-	51+	12000+
	9+	573750+	90769472+	7034+	3121-	51+	15000+

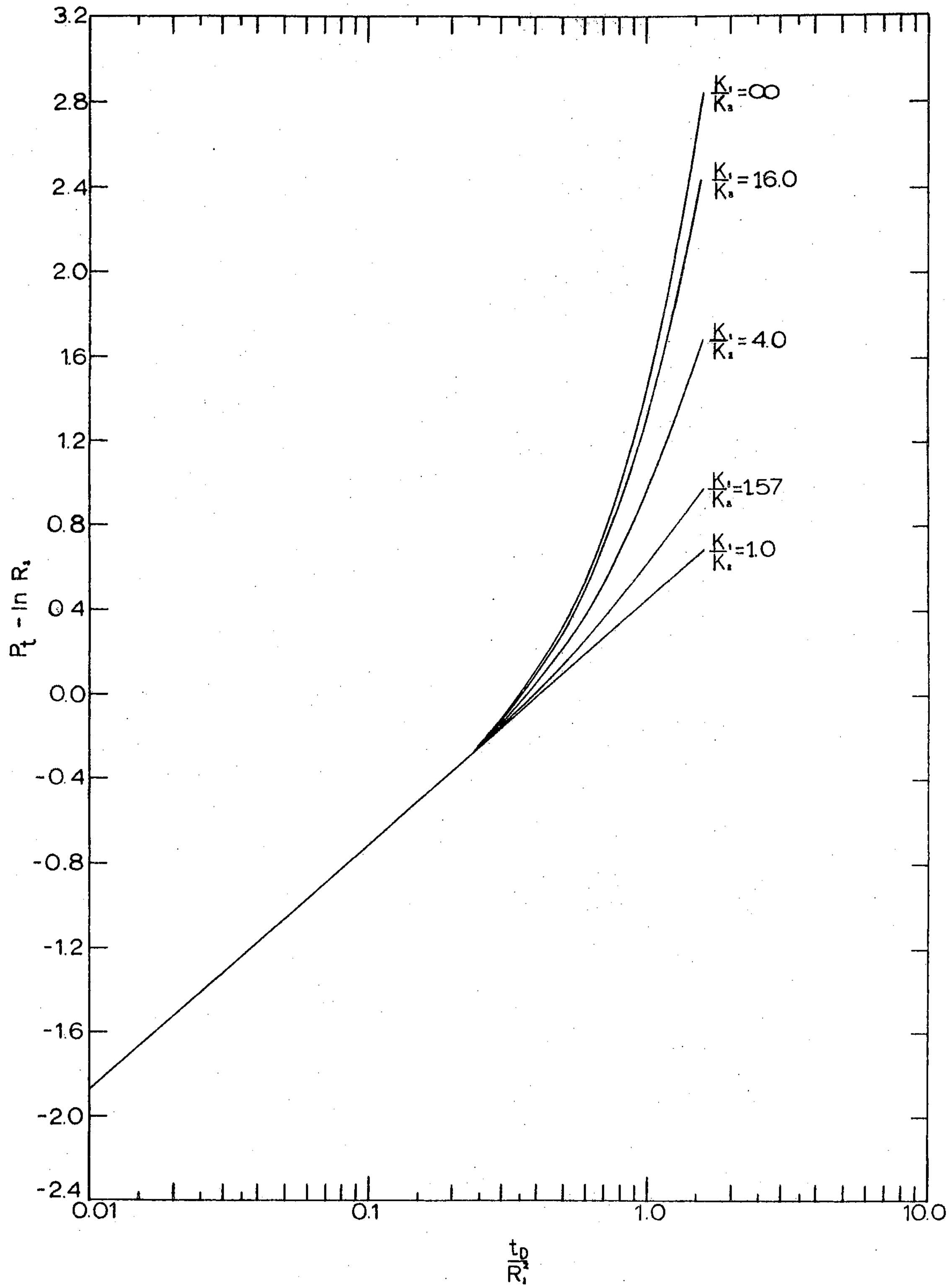

FIGURE 5 PRESSURE DRAW–DOWN CURVES

dimensionless pressure change functions for the plot were obtained from the calculated dimensionless pressure ratios by using equation (3-5).

The straight line portion of the curves represents the pressure draw-down that would occur if the entire reservoir had the same permeability as the inner zone. The effect of the outer permeability zone on the draw-down curve occurs when the curve deviates from a straight line.

CHAPTER VII

SUMMARY AND CONCLUSIONS

The purpose of this study was to develop a procedure for theoretically determining the effective fracture radius and the increase in effective permeability created by hydraulic fracturing a natural gas reservoir.

A fractured reservoir was approximated by assuming the reservoir was composed of two radial concentric zones of different permeabilities. Difference equations were developed to solve the flow equation for the system. By incorporating the difference equation into a computer program, dimensionless pressure ratios at the inner boundary of the reservoir were determined for the constant production rate case. The results were plotted on a coordinate system which gave the same set of curves for reservoirs with various inner zone radii.

The reservoir was initially assumed to have a uniform pressure. Then a constant flow rate was imposed across the inner boundary. The pressure transient created by the imposed flow rate moved outward in the reservoir with time. When the pressure transient reached the outer zone, the change in permeability resulted in a second transient being reflected back towards the inner boundary.

Before the second transient reached the inner boundary of the reservoir the pressure draw-down curve was determined by the permeability of the inner zone. The straight line portion of the curve represents the draw-down characteristics of a reservoir with a uniform permeability. This conclusion is illustrated by the curve for the case where the permeability ratio between the inner and outer zones is equal to one.

After the second pressure transient reached the inner boundary, the pressure draw-down curve deviated from a straight line. The amount of deviation depended upon the permeability ratio between the inner and outer zones.

The time required for a pressure transient to reach the outer zone and be reflected back was dependent upon the radius and permeability of the inner zone. From the draw-down curves, this time was determined to be equivalent to a t_D/R_1^2 value of 0.25. This relationship agrees with an equation developed by Cornell (4) to determine the dimensionless time at which the pressure draw-down curve for the finite reservoir case deviates from a straight line. The case of an infinite permeability ratio between the inner and outer zones is equivalent to the finite reservoir case.

From the analysis of the results, it was concluded that the permeability of the inner zone could be determined for the slope of the straight line portion of the draw-down curve. The procedure for calculating the effective permeability from draw-down curves has been presented by Cornell (2)(8). The procedure is discussed in Chapter II.

By determining the t_D value at which the draw-down curve deviated from a straight line, the radius of the inner zone can be calculated. The inner zone radius is obtained by multiplying the t_D value by 0.25. By using the coordinates of Figure 5 to draw a curve, the permeability of the outer zone can be estimated by comparing the curve with the plot in Figure 5. An example problem is worked in the Appendix.

The dimensionless groups used in developing the difference equations were for natural gas reservoirs. The results and curves apply equally as well to single phase production from oil reservoirs when dimensionless groups for oil reservoirs are used.

CHAPTER VIII

RECOMMENDATION FOR FUTURE STUDY

The draw-down pressures calculated in this study were for the constant production rate case in an infinite composite reservoir. Draw-down curves for the constant pressure case could be calculated using the procedure which has been presented. The case of a finite composite reservoir could also be investigated.

A closely related problem would be developing theory for pressure build-up curves in composite reservoirs. The finite difference procedure was extended to calculate pressure build-up curves; but, sufficient accuracy was not achieved. The equation developed by Loucks (9) could be evaluated on a computer to obtain pressure build-up curves.

By studying actual field tests, a comparison could be made between the pressure draw-down and build-up characteristics of fractured reservoirs and non-uniform mathematical reservoirs.

A SELECTED BIBLIOGRAPHY

1. Chatas, A. T.: "A Practical Treatment of Nonsteady-state Flow Problems in Reservoir Systems," Petroleum Engineer (May, 1953) 25, B42.

2. Cornell, David: "Permeability Determined from Production Data," World Oil (February, 1953) 136, 186.

3. Cornell, David, and Donald L. Katz: "Pressure Gradients in Natural Gas Reservoirs," Trans. AIME (1953), 198, 61.

4. Cornell, David: Personal Interview, May 16, 1961, at Oklahoma State University.

5. Darcy, H.: "Les Fontaines Publiques de la Ville de Dijon," Victor Dalmont, Paris (1856).

6. Hodgson, R. N., G. C. Clark, and M. D. Rowe: "Economic Optimization of a Development Program for a Low-Permeability Reservoir," Journal of Petroleum Technology (March, 1961), 13, 231.

7. Horner, D. R.: "Pressure Build-Up in Wells," Proceedings of Third World Petroleum Congress, Section II. Hague, (1951), 503.

8. Katz, D. L., et al: Handbook of Natural Gas Engineering. New York: McGraw-Hill, 1959, Chapters 10 and 11.

9. Loucks, Terry A.: "A Study of Pressure Build-Up in a System Composed of Two Adjacent Concentric Regions of Different Permeabilities," Tulsa, Master's Thesis, University of Tulsa, 1960.

10. Miller, C. C., A. B. Dyes, and C. A. Hutchinson: "The Estimation of Permeability and Reservoir Pressure from Bottom Hole Pressure Build-Up Characteristics," Trans. AIME (1950), 201, 91.

11. Mortada, M.: "Oilfield Interference in Aquifers of Non-Uniform Properties," Journal of Petroleum Technology (December, 1960), 12, 55.

12. Muskat, Morris: The Flow of Homogeneous Fluids Through Porous Media. New York: McGraw-Hill, 1937, 641.

13. Salvadori, M. G., and M. L. Baron: "Finite Differences and Their Applications," Numerical Methods in Engineering. Englewood Cliffs: Prentice-Hall, (1956).

14. Schneider, P. J.: Conduction Heat Transfer. Reading: Addison Wesley, (1955), 301.

15. Van Everdingen, A. F., and W. Hurst: "The Application of the Laplace Transformation to Flow Problems in Reservoirs," Trans. AIME (1949), 186, 305.

APPENDIX

The following problem was made up to illustrate the calculation procedure used for determining the radius of the inner zone and the permeabilities of both zones in a composite reservoir.

PROBLEM:

A fractured natural gas well which has been shut-in is produced at a constant flow rate of 500 Mcf/day. The original reservoir pressure was 800 psia. The bottom-hole pressures are shown in Table III. The known fluid and reservoir properties are as follows:

Reservoir temperature, T	$= 125^{o}F$
Porosity, ϕ	$= 0.20$
Reservoir thickness, h	= 17.0 feet
Viscosity, μ	= 0.022 centipoises
Well bore radius, r_w	= 0.25 feet

Determine the effective fracture radius and the permeability of the inner and outer zones.

SOLUTION:

A semilogarithmic plot of the draw-down data is constructed. Figure 6 shows this plot. By using equation (2-2), the permeability of the inner zone is determined from the slope of the first portion of the draw-down curve. The slope was found to be 6,100 $psia^2$ per time cycle.

TABLE III

EXAMPLE PROBLEM DRAW-DOWN DATA

Measurement Number	Time (hours)	Pressure (psia)
1	0.15	779.2
2	0.25	778.2
3	0.50	777.2
4	0.75	776.5
5	1.00	775.9
6	1.25	775.5
7	1.50	775.0
8	1.75	774.6
9	2.00	774.1
10	2.50	773.3
11	3.00	772.4
12	4.00	771.1
13	5.00	770.1
14	6.00	769.1
15	7.00	768.5
16	8.00	767.6

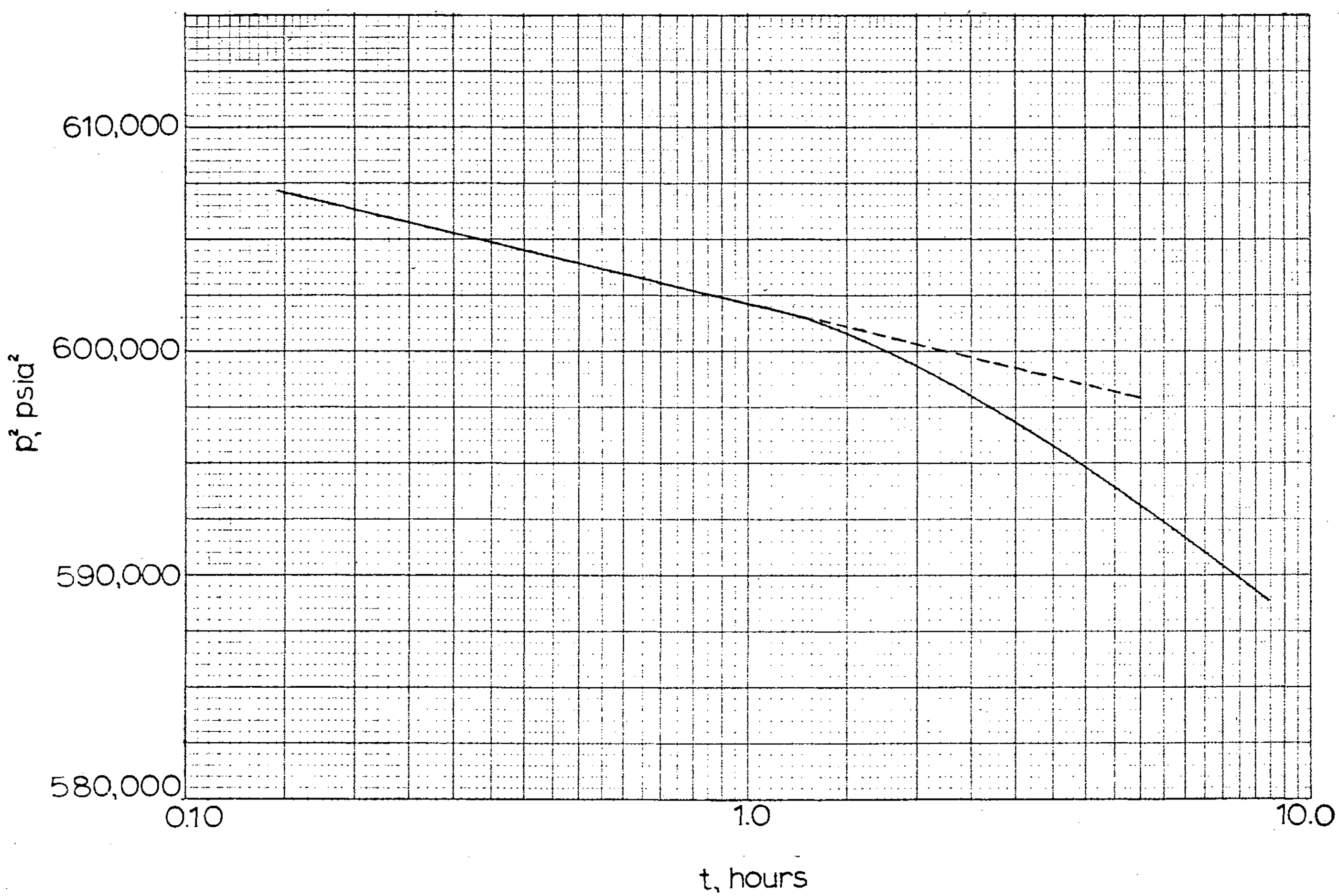

FIGURE 6   EXAMPLE PROBLEM DRAW-DOWN CURVE

$$K_1 = \frac{1,424\ \bar{\mu}\ \bar{Z}\ T\ Q}{2\ h\ S}$$

$$K_1 = \frac{1,424 \times 0.022 \times 0.89 \times 585 \times 500 \times 2.303}{2 \times 17 \times 6.1\text{x}10^3}$$

$$K_1 = 90.6 \text{ millidarcys}$$

To determine the radius of the inner zone, the dimensionless time at which the draw-down curve deviates from a straight line is first calculated. From Figure 6 the time the draw-down curve deviates from a straight line is 1.32 hours. By using equation (3-1) the dimensionless time is calculated.

$$t_D = \frac{2.634\text{x}10^{-4}\ t\ K\ \bar{p}}{\mu\ \phi\ r_w^{\ 2}}$$

$$t_D = \frac{2.634\text{x}10^{-4} \times 1.32 \times 90.6 \times 783.5}{0.022 \times 0.20 \times 0.0625}$$

$$t_D = 90,000$$

Knowing that the draw-down curve deviates from a straight line at a t_D/R_1^2 value of 0.25, the radius of the inner zone can be calculated.

$$R_1 = \left(\frac{t_D}{0.25}\right)^{\frac{1}{2}}$$

$$R_1 = 2(90,000)^{\frac{1}{2}}$$

$$R_1 = 600$$

By using equation (3-2) the inner zone radius in feet is obtained.

$$R = \frac{r}{r_w}$$

$$r = 600 \times 0.25$$

$$r = 150 \text{ feet}$$

The permeability of the outer zone is determined by making a plot shown by Figure 7. The P_t function for the plot is obtained from equations (3-3), (3-4) and (3-5). By comparing the curve in Figure 7 with the curves in Figure 5, the permeability ratio of the inner and outer zones was determined to be 4.0. Since the permeability of the inner zone has already been determined, the permeability of the outer zone can be calculated.

$$K_2 = \frac{K_1}{4.0}$$

$$K_2 = \frac{90.6}{4.0}$$

$$K_2 = 22.7 \text{ millidarcys}$$

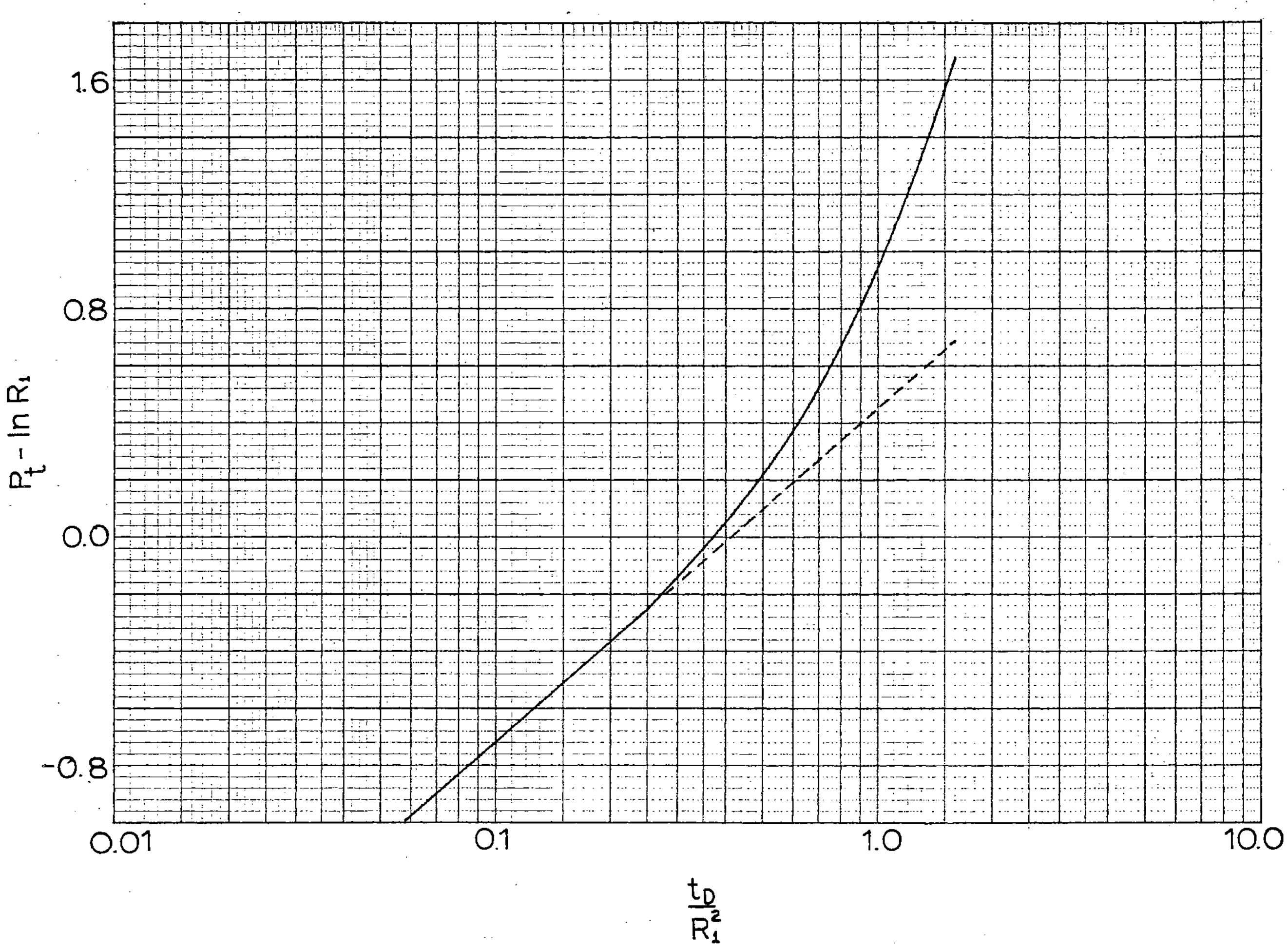

FIGURE 7 SHIFTED DRAW–DOWN CURVE

VITA

Roy Leonard Woods

Candidate for the Degree of

Master of Science

Thesis: UNSTEADY-STATE FLOW IN NON-UNIFORM PETROLEUM RESERVOIRS

Major Field: Mechanical Engineering

Biographical:

Personal Data: Born at Seiling, Oklahoma, September 20, 1937, the son of Ted G. and Sylvia C. Woods.

Education: Attended grade school at Seiling, Oklahoma; graduated from Seiling High School, Seiling, Oklahoma in 1955; received the Bachelor of Science degree from Oklahoma State University in January, 1960; completed requirements for the Master of Science degree in August, 1961.

Experience: Employed by the Halliburton Oil Well Cementing Company at Duncan, Oklahoma as an assistant machinist during the summer of 1957; employed by Mobil Oil Company in Healdton, Oklahoma during the summer of 1958 as a roustabout; employed by Humble Oil and Refining Company at Refugio, Texas, during the summer of 1959 as an engineering trainee; employed by Oklahoma State University as a teaching assistant from January, 1960, to June, 1960; employed by Shell Oil Company at Denver, Colorado during the summer of 1960 as a Jr. Mechanical Engineer.